Colloids and Surfaces A: Physicochem. Eng. Aspects 324 (2008) 35–40

Contents lists available at ScienceDirect

Colloids and Surfaces A: Physicochemical and Engineering Aspects

journal homepage: www.elsevier.com/locate/colsurfa

Foam films stabilized with alpha olefin sulfonate (AOS)

R. Farajzadeh [a], R. Krastev [b,*], P.L.J. Zitha [a,**]

[a] Delft University of Technology, Department of Geotechnology, Stevinweg 1, 2628 CN Delft, The Netherlands
[b] Max-Planck Institute of Colloids and Interfaces, 14424 Potsdam/Golm, Germany

ARTICLE INFO

Article history:
Received 13 November 2007
Received in revised form 15 March 2008
Accepted 20 March 2008
Available online 28 March 2008

Keywords:
Foam film
AOS surfactant
Monolayer
Film thickness
Surface tension
Adsorption
Ionic activity

ABSTRACT

Alpha olefin sulfonate (AOS) surfactants have shown outstanding detergency, lower adsorption on porous rocks, high compatibility with hard water and good wetting and foaming properties. These properties make AOS an excellent candidate for foam applications in enhanced oil recovery. This paper summarizes the basic properties of foam films stabilized by an AOS surfactant. The foam film thickness and contact angle between the film and its meniscus were measured as a function of NaCl and AOS concentrations. The critical AOS concentration for formation of stable films was obtained. The critical NaCl concentration for formation of stable Newton black films was found. The dependence of the film thickness on the NaCl concentration was compared to the same dependence of the contact angle experiments. With increasing NaCl concentration the film thickness decreases gradually while the contact angle (and, respectively the free energy of film formation) increases, in accordance with the classical DLVO theory.

The surface tension isotherms of the AOS solutions were measured at different NaCl concentrations. They coincide on a single curve when plotted as a function of mean ionic activity product. Our data imply that the adsorption of AOS is independent of NaCl concentration at a given mean ionic activity.

1. Introduction

Foam is a dispersion of a gas phase in a continuous liquid phase stabilized by surfactants and/or nano-particles [1,2]. In petroleum industry, to prevent the early gas breakthrough into the production wells gas is often injected together with a surfactant solution. In this way viscous foam is formed which controls the gas mobility and therefore enhances the sweep efficiency (i.e. the amount of recoverable oil) [3]. Foams are also excellent acid diversion agents and are widely used to block the water producing zones of the oil reservoirs [4,5].

The choice of surfactant with respect to the injected gas, type of the porous medium and chemical/physical properties of the fluids in the porous medium, e.g., oil is an important key in the success of a foam injection process. A suitable surfactant should be capable of generating ample and stable foam in the presence of reservoir rock and oil at high pressures and temperatures. Furthermore, a successful surfactant must have less adsorption on the rock. Adsorption of the surfactant on the rock surface decreases the surfactant concentration and therefore limits the distance the surfactant will propagate into the oil reservoir before its concentration becomes too low to be effective in generating the foam [6]. The stability of foam in the presence of oil (often regarded as an anti-foam) is another challenge in the application of foam as an enhanced oil recovery (EOR) method. In general, the selected surfactant in EOR foam has to balance chemical costs against the expected gas mobility reduction, taking into account surfactant adsorption and foam–oil interaction.

Alpha olefin sulfonate (AOS) surfactants have comparatively lower adsorption on sandstones [7]. Moreover, AOS surfactants provide outstanding detergency, high compatibility with hard water, and good wetting and foaming properties with CO_2 even when the porous medium is partially saturated with oil [8]. These properties make AOS surfactants an excellent candidate for (CO_2)-foam applications, e.g., EOR projects that aim to produce more oil from underground reservoirs.

When foam is injected to porous media the liquid lamella of the foam bridge the pore throats and consequently blocks some of the gas path flow [9]. In many cases the long-term stability of foam is directly related to the stability of the single separating liquid films lamella. Thus it is important to know the basic properties of the lamella that separate the gas bubbles.

Foam films are suitable tools for studying the interactions between interfaces [2,10]. Generally they are formed from solution of surfactants with or without electrolytes. There are two equilibrium states of foam films that are defined by the thermodynamic conditions. Common films are usually formed when the salt concentration in the film-forming solution is low. These films have a

* Corresponding author. Tel.: +49 3315679232.
** Corresponding author.
E-mail addresses: rumen.krastev@mpikg.mpg.de (R. Krastev), p.l.j.zitha@tudelft.nl (P.L.J. Zitha).

0927-7757/$ – see front matter © 2008 Elsevier B.V. All rights reserved.
doi:10.1016/j.colsurfa.2008.03.024

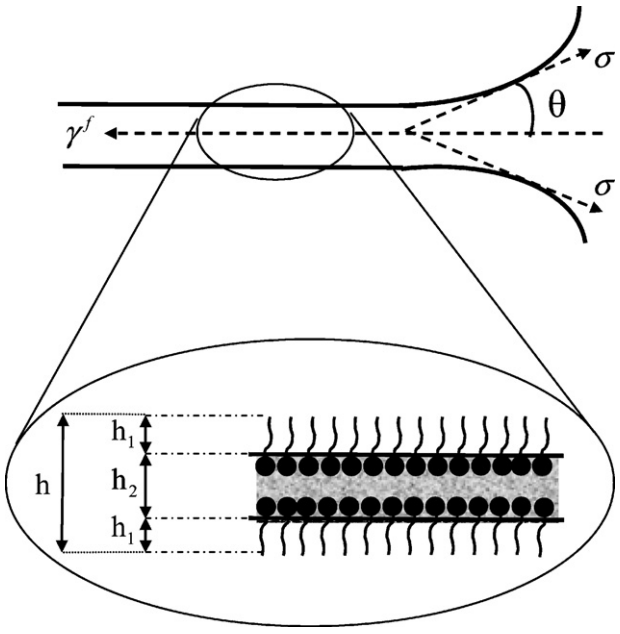

Fig. 1. A single foam film consists of an aqueous core with thickness h_2 sandwiched between two adsorbed monolayers of surfactant with the thickness of h_1. The liquid and monolayers are assumed to be homogenous. The contact angle, θ, is formed at the transition between the film and the bulk solution.

sandwich-like structure (Fig. 1) and consist of two monolayers of adsorbed surfactant molecules stabilizing the film separated by an aqueous layer. The film thickness decreases when the salt concentration in the film-forming solution increases. The reflectivity from the film decreases so much at certain film thickness (respectively, high salt concentration) that the films look black in reflected light. These films are called common black films (CBF). The interactions in these films are described by the classical DLVO approach [11]. Their stability is due to the interplay between the repulsive electrostatic (Π_{EL}) and the attractive van der Waals (Π_{vw}) component of the disjoining pressure, Π. The Π_{EL} decreases with the further addition of salt to the film-forming solution until it is fully suppressed. Very thin Newton black films (NBF) are formed at that point. These films have bilayer structures: the two surfactant monolayers are close to each other, separated only by few layers of hydration water. The stability of these films is governed by the interplay of the short-range interaction forces. The application of DLVO theory to such thin foam films is limited because the theory does not take into account the short-range forces operating between the film interfaces [10,12,13]. In both cases the transition from thicker common film to the thinner black films (either CBF or NBF) occurs through the formation of black spots in the thicker film.

In this paper we study the properties of foam films prepared from AOS solutions in presence of different amounts of electrolyte (NaCl). The thickness and contact angle of the films were measured. Complementary studies on surface tension of AOS surfactant solutions were performed for better understanding of the results. Thus, the surface density of the surfactant in their adsorption layers on water surface was estimated.

2. Materials and methods

2.1. Surface tension

The surface tension was measured using a K11 tensiometer (Krüss GmbH, Germany) applying the DuNouy ring method. The solutions were prepared at least 12 h prior to the experiments and sonicated for 30 min. The solutions remained still in the Teflon vessels for 2 h before the measurements to assure the equilibrium adsorption at the liquid/air surface and for at least 30 min between every single measurement to recover the equilibrium.

2.2. Foam film experiments

The experiments were performed in a Scheludko–Exerowa ring cell [2,14] with an inner radius of the ring (R_{cap}) of 2.5 mm. Detailed description of the cell and the used experimental procedures are given in Ref. [2,15]. The ring cell was placed in a closed thermostat vessel saturated with vapor of the studied solution. Two hours were allowed for the attainment of equilibrium before the measurement was started. A horizontal microscopic film with constant radius was formed in the glass ring, by suction of the film-forming solution from the ring through the capillary at a low capillary pressure. The film starts thinning after its formation due to drainage. It either ruptures during the thinning process or an equilibrium film is formed at the end of the drainage process.

2.2.1. Film thickness

The equivalent solution film thickness h_w was measured microinterferometrically [2,14–16] by assuming an optically homogeneous film with the same refractive index n as that of the bulk solution from which the film was formed.

$$h_w = \frac{\lambda}{2\pi n} \arcsin\sqrt{\frac{I/I_m}{1 + 4R_h/(1-R_h)^2(1-I/I_m)}} \quad (1)$$

where $R_h = (n-1)^2/(n+1)^2$, λ is the wavelength of the light (in this study 546 nm), I_m and I are the maximum intensity of the light and the intensity of the light reflected from the film at each moment during the thinning process or in equilibrium.

In fact the film consists of two surfactant monolayers and an aqueous layer in between. Thus, the film thickness h is different from that of h_w. The film thickness h was calculated by assuming a three-layer model of the film [16] where the aqueous solution core of thickness h_2 and refractive index n_2, is flanked by two layers of hydrophobic alkyl chains of the adsorbed surfactant molecules, with thickness h_1 and refractive index n_1. The aqueous core includes the hydrophilic head groups of the surfactant molecules. This three-layer model was used to calculate the film thickness h from the experimentally obtained h_w values using the relation [16]:

$$h = 2h_1 + h_2; \quad h_2 = h_w - 2h_1\frac{n_1^2 - 1}{n_2^2 - 1} \quad (2)$$

The correction is especially important for thin NBFs. We assumed that the thickness h_1 = 1.35 nm [17] as used for similar films and the refractive index n_1 as that of pure tetradecane n_1 = 1.4290 [18].

2.2.2. Contact angle

The contact angle between the film and bulk solution, θ, (Fig. 1) was measured by the expansion method at constant pressure [19]. During the drainage process, due to the local fluctuations of the film thickness black spots appear. These spots grow and finally cover the whole film. The film expands shortly (in less than a second) at that moment because of the new force balance between the film and the bulk meniscus. Thereafter the film size remains constant without any further change. The radius of the thinner equilibrium black film r_2 is greater than the radius of the thicker film r_1 just before the first black spot appears. The contact angle was evaluated using the

relation [19]

$$\sin\theta = \frac{\delta_2^2 - \delta_1^2}{\delta_2} \quad (3)$$

where $\delta_1 = r_1/R_{cap}$ and $\delta_2 = r_2/R_{cap}$. This calculation is based on the estimation of the pressure in the system foam film/meniscus before and after the film expansion, which supplement the formation of the black films and the assumption that this pressure does not change during the film transition. It should be mentioned that the method is more precise when $\theta > 1^\circ$.

All measurements (thickness, contact angle and surface tension) were conducted at room temperature ($T = 25 \pm 0.5\,^\circ$C) and every point presented is average of at least 10 single measurements. The standard deviation is less than 5% of the mean values.

2.3. Materials

The surfactant used was (C_{14}–C_{16})-alpha-olefin sulfonate, AOS (Stepan Company, USA). This surfactant is anionic, with industrial purity and was used as received without any further purification. The general structure of olefin surfactants is R-$SO_3^-Na^+$, where R represents the hydrophobic alkyl group. In our case, the number of the carbon atoms in the surfactant structure is between 14 and 16 and the molecular weight of the surfactant is $M_w \approx 315$. Sodium chloride (NaCl) GR grade (Merck, Darmstadt, Germany) was roasted at 600 °C for 5 h to remove the organic impurities, some of which might be surface active. All solutions were prepared with deionized water from a Milli-Q purification setup (Elga Labwater, Germany). The specific resistance of the water was 18.2 MΩ cm, the pH was 5.5 and the total organic carbon (TOC) value was <10 ppb.

3. Results and discussion

3.1. Surface tension

The measured surface tension isotherms for different concentrations of the added electrolyte, NaCl, are presented in Fig. 2. The surface tension decreases with increasing surfactant concentration for all electrolyte concentrations until it reaches a minimum. The existence of a minimum in the curves indicates that the surfactant contains diverse surface-active molecules with different activity or contains some impurities. The surface tension values increase slightly after this minimum and remain constant afterwards. The addition of NaCl does not change the slope of the curve but only shifts them toward lower values of the surfactant concentrations. This means that the critical micelle concentration (CMC) decreases with increasing NaCl concentration, as shown in Table 1. A similar behavior has been reported for other ionic surfactant-electrolyte systems [20–22].

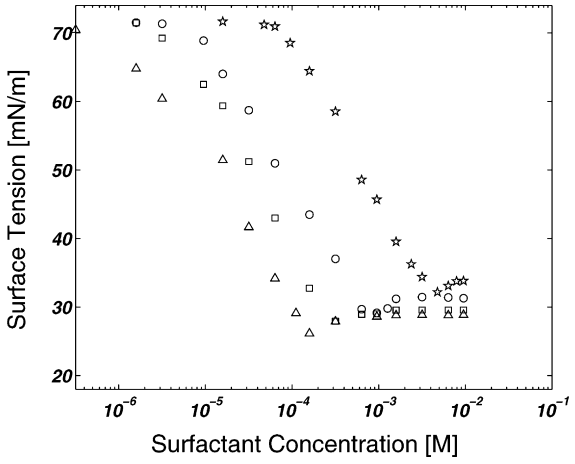

Fig. 2. The measured surface tension isotherms ($T = 25\,^\circ$C) vs. surfactant concentration with different NaCl concentrations: (*) no salt, (◯) $c_{NaCl} = 0.5$ M, (□) $c_{NaCl} = 0.2$ M and (△) $c_{NaCl} = 0.5$ M. The addition of NaCl alters the shape of the curves. Higher amount of NaCl shifts the surface tension curves to lower surfactant concentrations.

Table 1
CMC values of AOS solutions at different NaCl concentrations obtained from the surface tension isotherms presented in Fig. 2

NaCl concentration (M)	CMC (wt.% AOS)
0.50	0.004
0.20	0.007
0.05	0.018
0.00	0.100

We followed the thermodynamic method explained in Ref. [21] to determine the adsorption of the surfactant at liquid/air interface, which is an extension of the approach of Rehfeld [23]. According to the theory the Gibbs adsorption isotherm in a suitable form, which accounts for the added inorganic salt is given by

$$\Gamma_s = -\frac{1}{RT}\left(\frac{d\sigma}{d\ln(aa_t)}\right)_T \quad (4)$$

here R is the universal gas constant, T is temperature, σ is the measured surface tension and a and a_t are the activities of the ionic AOS or surfactant + electrolyte (AOS + NaCl) solutions, respectively defined by

$$a = \gamma_\pm c_{AOS} \quad \text{and} \quad a_t = \gamma_\pm(c_{AOS} + c_{NaCl}) \quad (5)$$

with $\gamma_\pm$ the mean ionic activity coefficient. An equation accurately representing measured values of $\gamma_\pm$, up to 2 M solutions of NaCl is provided by Debye–Hückel formula corrected for short-range interactions [24,25]

$$\log\gamma_\pm = -\frac{0.5115\sqrt{I}}{1 + 1.316\sqrt{I}} + 0.055I \quad (6)$$

where I is the ionic strength in moles and the numerical constants correspond to 25 °C. For consistency sake we also define so-called "mean ionic activity" as

$$c^* = (aa_t)^{1/2} = \gamma_\pm(c_{AOS}(c_{AOS} + c_{NaCl}))^{1/2} \quad (7)$$

Eq. (4) suggests a way to determine the adsorption from the surface tension measurements. Gurkov et al. [21] proposed that the isotherm of σ versus $\ln(aa_t)$ can be fitted with a polynomial function

$$\sigma = z_0 + z_1\ln(aa_t) + z_2(\ln(aa_t))^2 + z_3(\ln(aa_t))^3 + \cdots \quad (8)$$

Therefore, to determine the adsorption we fitted our measured surface tension data to a quadratic function (for example see Fig. 3) and calculated the adsorption using Eq. (4).

Fainerman and Lucassen-Reynders [22,26] pointed out that for solutions of a single ionic surfactant with inorganic electrolyte the measurements of surface tension (or surface pressure) versus mean ionic activity (c^*) at different electrolyte concentrations coincide on a single curve. The measured surface tension data of AOS solutions are presented in Fig. 4 as a function of the mean ionic activity (c^*). The isotherms of σ pass through a master curve for different NaCl concentrations, except for the solution without NaCl. This implies that at a given mean ionic activity, both adsorption and surface tension are independent of electrolyte concentration, i.e. the ionic atmosphere contribution to the surface pressure is negligible. This is confirmed in Fig. 5 where the calculated adsorptions are plotted versus mean ionic activity, c^*. The adsorption Γ_s, continuously increases with the addition of either salt or surfactant by c^*. The complete absence of inert electrolyte in the studied solutions

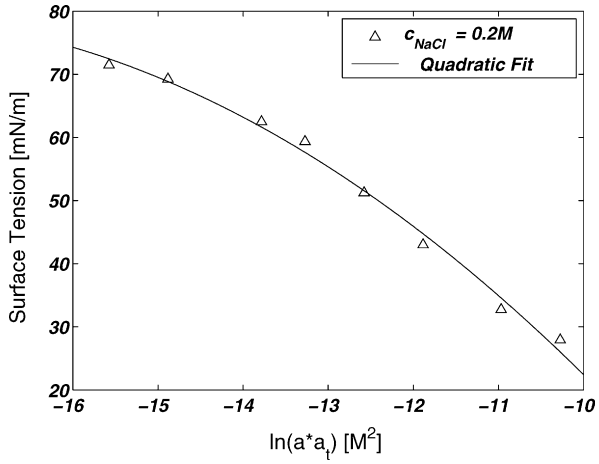

Fig. 3. Surface tension isotherms in presence of 0.2 M NaCl vs. $\ln(aa_t)$. The experimental points (△) are fitted to a quadratic function according to Eq. (8). The equation of the solid line reads $\sigma = -0.78[\ln(aa_t)]^2 - 28.8\ln(aa_t) - 188.2$ and the correlation coefficient of the fit is $R^2 = 0.996$.

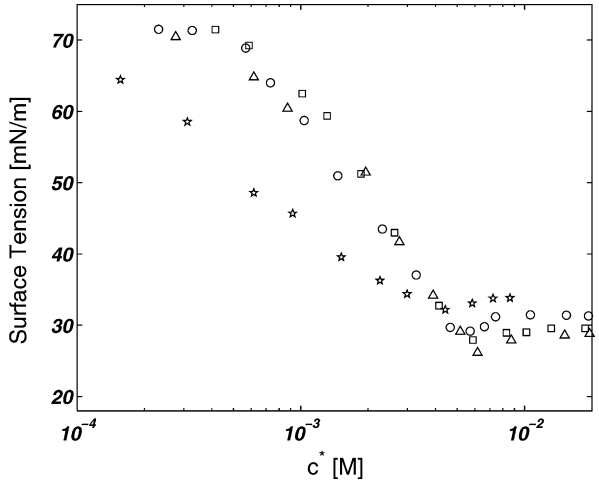

Fig. 4. The measured surface tension isotherms ($T = 25\,^\circ$C) vs. mean ionic activity c^*. (*) no salt, (○) $c_{NaCl} = 0.05$ M, (□) $c_{NaCl} = 0.2$ M and (△) $c_{NaCl} = 0.05$ M. All curves with NaCl follow a master curve.

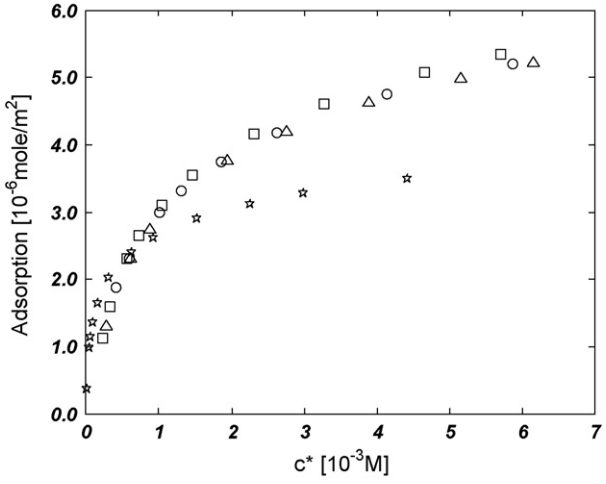

Fig. 5. Calculated adsorption, Γ_s, vs. mean ionic activity for AOS solutions and different NaCl concentrations: (*) no salt, (○) $c_{NaCl} = 0.05$ M, (□) $c_{NaCl} = 0.2$ M and (△) $c_{NaCl} = 0.5$ M Γ_s is less for the solution without NaCl compared to the solution with NaCl. Γ_s is independent of NaCl concentration at a given c^*.

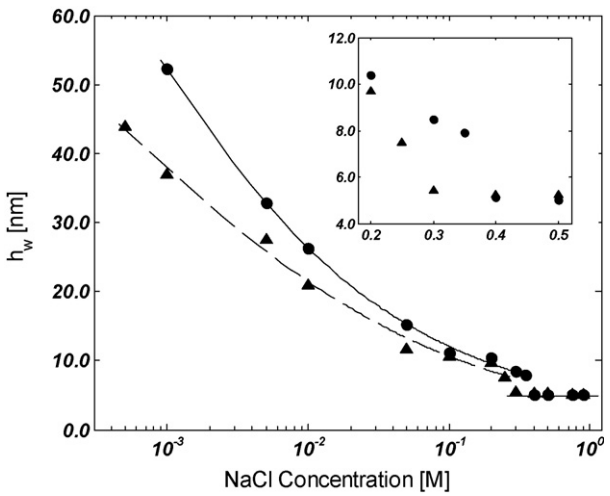

Fig. 6. Dependence of the experimentally obtained equivalent film thickness, h_w, on NaCl concentration for constant AOS concentrations of (●) $c_{AOS} = 0.01$ wt.% (3×10^{-4} M) and (▲) $c_{AOS} = 0.3$ wt.% (9.5×10^{-3} M) at a constant temperature of $T = 25\,^\circ C$. The concentrations in which the transition from CBF to NBF happens are more clear in the inset. The solid (—) and dashed (- - -) lines are only guides for the eyes.

results in an adsorption curve very different from that in presence of salt. The adsorption is lower in this case. Similar effect was already observed in Ref. [21] and the authors attributed it to "enhanced electrostatic screening in the double layer and decreased repulsion between the surfactant ions" upon addition of salt.

3.2. Foam film experiments

The dependence of the equivalent solution film thickness h_w on the NaCl concentration was investigated for two surfactant concentrations, one ($c_{AOS} = 0.01$ wt.% $= 3 \times 10^{-4}$ M) below and the other ($c_{AOS} = 0.3$ wt.% $= 9.5 \times 10^{-3}$ M) above the CMC of the AOS solution in the absence of NaCl. The results are shown in Fig. 6 and the calculated h and h_2 are summarized in Table 2. Thick films are formed at low salt concentration. The thickness of these films depends on the AOS concentration in the solution. Those made from AOS solutions with a concentration of 0.01 wt.% are thicker than those prepared in presence of 0.3 wt.% solution. This is because the AOS surfactant is an electrolyte itself and at low salt concentration its concentration determines the ionic strength of the solutions. Following the classi-

Table 2
Foam film thickness, h, and the thickness of the aqueous core, h_2 as a function of the NaCl concentration for films prepared from AOS solutions with concentrations $c_{AOS} = 0.01$ wt.% (3×10^{-4} M) and $c_{AOS} = 0.3$ wt.% (9.5×10^{-3} M)

c_{NaCl} (M)	$c_{AOS} = 0.01$ wt.% (3×10^{-4} M)		$c_{AOS} = 0.3$ wt.% (9.5×10^{-3} M)	
	h (nm)	h_2 (nm)	h (nm)	h_2 (nm)
0.0005			43.8	40.2
0.001	51.5	47.9	36.9	32.3
0.005	32.9	29.3	27.4	23.8
0.01	26.3	22.7	20.9	17.3
0.05	15.3	11.7	11.7	8.1
0.10	11.1	7.4	10.6	7.0
0.20	10.3	6.7	9.7	6.0
0.25	8.4	4.8	7.5	3.8
0.30			5.4	1.8
0.35	7.9	4.3		
0.40	5.1	1.5	5.2	1.6
0.50	5.0	1.4	5.2	1.6
0.75	5.0	1.4	5.1	1.5
0.90	5.0	1.4	5.1	1.5

The thicknesses were calculated from the experimentally obtained h_w using Eq. (2).

Table 3
Values of the contact angle, θ, the surface tension, σ and the specific interaction film free energy, Δg^f as a function of NaCl concentration for two surfactant concentrations

c_{NaCl} (M)	c_{AOS} = 0.01 wt.% (3×10^{-4} M)			c_{AOS} = 0.3 wt.% (9.5×10^{-3} M)		
	θ (deg)	σ (mN/m)	Δg^f (mJ/m^2)	θ (°)	σ (mN/m)	Δg^f (mJ/m^2)
0.20	0.5	27.5	-2.2×10^{-3}	0.6	29.1	-2.8×10^{-3}
0.25	0.6	28.5	-3.0×10^{-3}	0.7	29.0	-4.7×10^{-3}
0.30	0.7	28.6	-4.0×10^{-3}	0.7	28.8	-4.3×10^{-3}
0.35	3.1	28.8	-4.9×10^{-3}	0.8	28.7	−0.09
0.40	4.0	28.6	−0.14	4.6	28.5	−0.18
0.50	4.7	27.5	−0.19	5.3	28.4	−0.24
0.70	6.0	28.4	−0.31	6.2	28.4	−0.33

cal DLVO theory the electrostatic double layer repulsion is weaker when the salt concentration is higher.

In both cases the film thickness decreases smoothly with increasing NaCl concentration. In the case of c_{AOS} = 0.001 wt.% CBF with an equivalent thickness of 11.1 nm are formed when concentration of NaCl is between 0.10 and 0.30 M while in the case of c_{AOS} = 0.3 wt.% CBFs with an equivalent thickness of 11.7 nm are formed when concentration of NaCl is between 0.05 and 0.20 M. The film thickness is 5.1 nm in the case of c_{AOS} = 0.01 wt.% above c_{NaCl} = 0.4 M and in the case of c_{AOS} = 0.3 wt.% above c_{NaCl} = 0.3 M and it is independent of NaCl and surfactant concentrations. We identify these films as NBFs which consist of two hydrophobic hydrocarbon layers of molecules with a thickness of about 1.35 nm and a core of bound water which includes the hydrophilic head groups of the AOS molecule with a thickness of 1.4 nm.

The critical concentration of formation of NBF is similar to that reported for other ionic surfactant like the classical sodium dodecylsulphate (SDS) which is 0.25 M of NaCl [27,28], but it is much higher than that reported for some non-ionic surfactants. For example it is 0.05 M NaCl for β-dodecyl maltoside. The transition concentration of NaCl above which only NBF are formed is higher in the case of the lower surfactant concentration (c_{AOS} = 0.01 wt.%). This is a result of the contribution of the surfactant ions and counter ions to the total electrolyte concentration of the solutions.

The dependence of the thickness of the foam films on the AOS concentration was also investigated at fixed NaCl concentration of c_{NaCl} = 0.50 M. The equivalent film thickness remained constant (with the average value of 5.1 nm) for all surfactant concentrations above c_{AOS} = 0.003 wt.% (9.5×10^{-5} M). Formation of stable films below this concentration was not possible.

The contact angle, θ, was measured for two surfactant concentration while the NaCl concentration was varied between 0.2 and 0.7 M. The results are shown in Fig. 7. For CBFs the contact angle is less than $\theta < 1°$. It increases with increasing NaCl concentration for both cases until it faces a jump. This jump is usually accepted as an indication of formation of NBFs [2,19,30]. The jump is between c_{NaCl} = 0.35 and 0.40 M for c_{AOS} = 0.01 wt.% and between c_{NaCl} = 0.30 and 0.35 M for c_{NaCl} = 0.3 wt.% which proves the transition from CBF to NBF. After the well-pronounced jump in the curves, the contact angle increases slower further. This indicates changes in the interactions between the film surfaces even after the formation of the NBF. It might be attributed to a further decrease in the electrostatic component of the disjoining pressure in this range of salt concentrations as already shown for films prepared from SDS in presence of NaCl [29].

When the two film surfaces approach each other the surface forces cause appearance of a disjoining pressure (Π) in the film [30]. It is related to the film tension γ^f (see Fig. 1) by

$$\gamma^f = 2\sigma - \int_{\infty}^{h} \Pi \, dh + \Pi h = 2\sigma + \Delta g^f + \Pi h \quad (9)$$

The free energy of film formation, Δg^f, provides useful information for studying the interaction forces in the films [30]. Usually, the term Πh is some orders of magnitude smaller that Δg^f and can be neglected. The forces balance in lateral direction at the line of intersection (see Fig. 1) requires that

$$2\sigma \cos\theta = \gamma^f \quad (10)$$

Combining (9) and (10) one obtains the following equation which relates Δg^f to the easy accessible experimentally contact angle:

$$\Delta g^f = 2\sigma(\cos\theta - 1) \quad (11)$$

The dependence of Δg^f on the NaCl concentration is presented in Table 3. The free energy of film formation has small value at low electrolyte concentrations. It increases sharply at a certain NaCl concentration. Similar to the contact angle behavior the jump is between c_{NaCl} = 0.35 and 0.40 M for c_{AOS} = 0.01 wt.% and between c_{NaCl} = 0.35 and 0.30 M for c_{AOS} = 0.3 wt.%. The increase in the absolute value of Δg^f emphasizes the fact that with increasing electrolyte concentration the contribution of the electrostatic repulsive forces (Π_{EL}) to the total film interaction free energy decreases and the formation of NBF from the initially formed CBF is energetically favorable process. The values of the specific interaction free energies are lower compared to that of films prepared from SDS. For example, it is −0.9 mJ/m^2 at 0.5 M NaCl in the film formed from SDS compared to ca. −0.20 mJ/m^2 depending on the surfactant concentration in the case of AOS stabilized films. This comparison shows that formation of NBF stabilized with SDS is energetically favorable than in the case of AOS stabilized films.

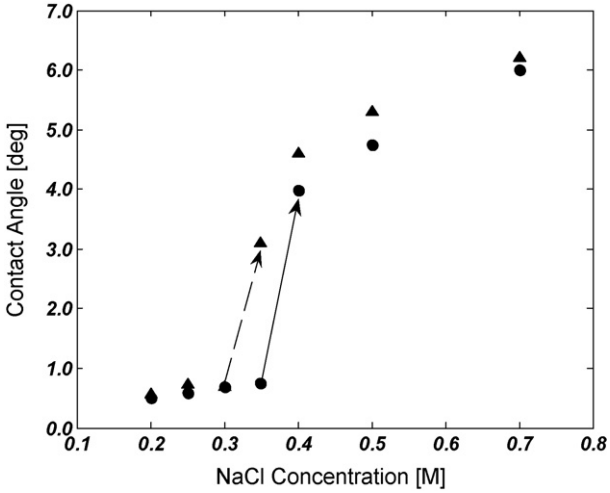

Fig. 7. Dependence of the contact angle between the film-forming solution and the film meniscus, θ, on NaCl concentration for constant AOS concentrations of (●) c_{AOS} = 0.01 wt.% (3×10^{-4} M) and (▲) c_{AOS} = 0.3 wt.% (9.5×10^{-3} M). The temperature is constant (T = 25 °C). The solid (—) and dashed (- - -) arrows are only guides for the eyes and show the jump in contact angle.

4. Conclusions

We calculated the adsorption of AOS surfactant at air/water interface using the surface tension data. It was shown that, except for the solution without salt, the addition of salt does not alter the adsorption Γ_s. Moreover, we studied the properties of foam films stabilized by AOS. It was observed that the films are not stable when $c_{AOS} < 0.03$ wt.% at a fixed concentration of $c_{NaCl} = 0.5$ M. The film thickness and contact angle, which is formed at the transition between the film and the bulk solution, were measured as a function of NaCl and surfactant concentration. The film thickness decreases with addition of NaCl due to the screening of the repulsive forces. The concentrations in which the NBFs are formed were also determined. Measurements of contact angle were used to calculate the free energy, Δg_f of film formation. The results show that Δg_f changes even when the conditions for the formation of NBF with constant thickness are achieved. This implies that the formation of NBF itself is not a state, which ensures the minimum in the film energy will be reached.

Acknowledgements

The authors are gratefully thankful to R. Nicolaes and S. Stöckle for their help in conducting experiments. Max-Planck Society is acknowledged for the partial support of the research stay of R. Farajzadeh at the MPI of Colloids and Interfaces in Golm, Germany.

References

[1] B.P. Binks, T.S. Horozov, Angew. Chem. 117 (2005) 3788.
[2] D. Exerowa, P.M. Kruglyakov, Foam and Foam Films, Elsevier Science, 1998.
[3] W.R. Rossen, in: R.K. Prud'homme, S.A. Khan (Eds.), Foams, Theory, Measurements and Application, Marcel Dekker, Inc., New York, 1996, pp. 413–463.
[4] F. Farshbaf Zinati, R. Farajzadeh, P.L.J. Zitha, Presented at European Formation Damage Conference, The Hague, The Netherlands, 2007, SPE 107790.
[5] P.Q. Nguyen, Dynamics of foam in porous media, Ph.D. Dissertation, Delft University of Technology, The Netherlands, 2004.
[6] J. Prieditis, G.S. Paulett, Presented at SPE/DOE Eighth Symposium on Enhanced Oil Recovery, Tulsa, Oklahoma, 1992, SPE 24178.
[7] D.X. Du, Personal Communication, 2007.
[8] R. Farajzadeh, D.X. Du, P.L.J. Zitha, unpublished data, 2007.
[9] D. Cohen, T.W. Patzek, C.J. Radke, Transp. Porous Media 28 (1997) 253.
[10] J. Israelachvili, Intermolecular and Surface Forces, Academic Press, London, 1991.
[11] B.V. Derjaguin, L.D. Landau, Acta Physicochem. USSR 14 (1941) 633; E.J.W. Verwey, J.Th.G. Overbeek, Theory of Stability of Liyophobic Colloids, Elsevier Pub. Co., N.Y., 1948.
[12] V. Bergeron, Langmuir 13 (1997) 3474.
[13] J. Israelachvili, H. Wennerstrom, J. Phys. Chem. 96 (1992) 520.
[14] A. Scheludko, Adv. Colloid Interface Sci. 1 (1967) 391.
[15] J.L. Toca-Herrera, H.J. Müller, R. Krustev, D. Exerowa, H. Möhwald, Colloids Surf. A 144 (1998) 319.
[16] S.P. Frankel, K.J. Mysels, J. Appl. Phys. 81 (1966) 3725–3748; E.M. Duyvis, The equilibrium thickness of free liquid films, Ph.D. Thesis, Utrecht University, 1962.
[17] J. Benattar, A. Schalchli, O. Belorgey, J. Phys. I France 2 (1992) 955.
[18] D. Lide (Ed.), Handbook of Chemistry and Physics, 73rd ed., CRC Press Inc., Cleveland, OH, 1993.
[19] T. Kolarov, A. Scheludko, D. Exerowa, Trans. Faraday Soc. 64 (1968) 2864; R. Krustev, H.-J. Müller, J.L. Toca-Herrera, Colloid Polym. Sci. 276(1998) 518.
[20] A.J. Prosser, E.I. Franses, Colloids Surf. A: Physicochem. Eng. Aspects 178 (2001) 1–40.
[21] T.D. Gurkov, D.T. Dimitrova, K.G. Marinova, C. Bilke-Crause, C. Gerber, I.B. Ivanov, Colloids Surf. A: Physicochem. Eng. Aspects 261 (2005) 29.
[22] V.B. Fainerman, E.H. Lucassen-Reynders, Adv. Colloid Interface Sci. 96 (2002) 295.
[23] S.J. Rehfeld, J. Phys. Chem. 71 (1967) 738.
[24] R.A. Robinson, R.H. Stokes, Electrolyte Solutions, Butterworths, London, 1959.
[25] E.A. Moelwyn-Hughes, Physical Chemistry, Pergamon Press, London, 1961.
[26] V.B. Fainerman, R. Miller, E.V. Aksenenko, A.V. Makievski, in: V.B. Fainerman, D. Mobius, R. Miller (Eds.), Surfactants: Chemistry, Interfacial Properties, Applications, Elsevier, Amsterdam, 2001, p. 189 (chapter 3).
[27] M.N. Jones, K. Mysels, P.C. Scholten, Trans. Faraday Soc. 62 (1966) 1336.
[28] H.G. Bruil, Specific Effects in Free Liquid Films, Meded, vol. 70–9, Landbouwhogescholl, Wageningen, 1970.
[29] N.C. Mishra, R.M. Muruganathan, H.-J. Müller, R. Krustev, Colloids Surf. A 256 (2005) 77.
[30] J.A. De Feijter, in: I. Ivanov (Ed.), Thin Liquid Films, Surfactant Science Series, vol. 29, Marcel Dekker, New York, 1988, pp. 1–47.